



UNIVERSITÀ
DEGLI STUDI
DI PADOVA

Università degli Studi di Padova

Padua Research Archive - Institutional Repository

Stable and Conserved G-Quadruplexes in the Long Terminal Repeat Promoter of Retroviruses

Original Citation:

Availability:

This version is available at: 11577/3307477 since: 2020-05-09T10:15:34Z

Publisher:

AMER CHEMICAL SOC

Published version:

DOI: 10.1021/acsinfecdis.9b00011

Terms of use:

Open Access

This article is made available under terms and conditions applicable to Open Access Guidelines, as described at <http://www.unipd.it/download/file/fid/55401> (Italian only)

(Article begins on next page)

Stable and Conserved G-Quadruplexes in the Long-Terminal-Repeat Promoter of Retroviruses

Emanuela Ruggiero,[†] Martina Tassinari,[†] Rosalba Perrone,[‡] Matteo Nadai,[†] and Sara N. Richter^{*,†}

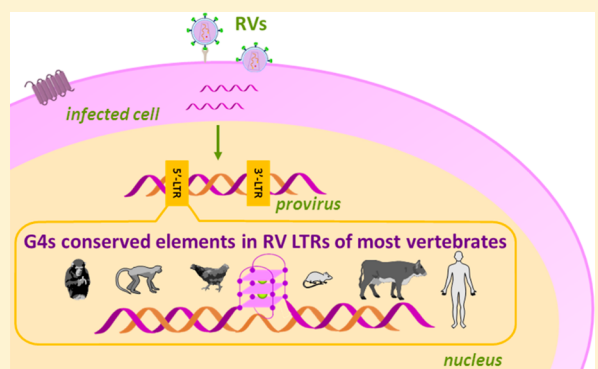
[†]Department of Molecular Medicine, University of Padua, via Aristide Gabelli 63, 35121 Padua, Italy

[‡]Buck Institute for Research on Aging, 8001 Redwood Boulevard, Novato, California 94945, United States

S Supporting Information

ABSTRACT: Retroviruses infect almost all vertebrates, from humans to domestic and farm animals, from primates to wild animals, where they cause severe diseases, including immunodeficiencies, neurological disorders, and cancer. Nonhuman retroviruses have also been recently associated with human diseases. To date, no effective treatments are available; therefore, finding retrovirus-specific therapeutic targets is becoming an impelling issue. G-Quadruplexes are four-stranded nucleic acid structures that form in guanine-rich regions. Highly conserved G-quadruplexes located in the long-terminal-repeat (LTR) promoter of HIV-1 were shown to modulate the virus transcription machinery; moreover, the astonishingly high degree of conservation of G-quadruplex sequences in all primate lentiviruses corroborates the idea that these noncanonical nucleic acid structures are crucial elements in the lentiviral biology and thus have been selected for during evolution. In this work, we aimed at investigating the presence and conservation of G-quadruplexes in the Retroviridae family. Genomewide bioinformatics analysis showed that, despite their documented high genetic variability, most retroviruses contain highly conserved putative G-quadruplex-forming sequences in their promoter regions. Biophysical and biomolecular assays proved that these sequences actually fold into G-quadruplexes in physiological concentrations of relevant cations and that they are further stabilized by ligands. These results validate the relevance of G-quadruplexes in retroviruses and endorse the employment of G-quadruplex ligands as innovative antiretroviral drugs. This study indicates new possible pathways in the management of retroviral infections in humans and animal species. Moreover, it may shed light on the mechanism and functions of retrovirus genomes and derived transposable elements in the human genome.

KEYWORDS: retroviruses, G-quadruplex, genome structure, LTR promoter, conservation



Retroviruses (RVs) are the most ancient known viruses: their origin dates back to more than 450 million years ago.¹ They are multifaceted viruses: they infect almost all vertebrates, ranging from humans to small animals (e.g., domestic cats and mice), farm animals (e.g., poultry, cattle, and goats), different primates, and other animals (e.g., horses and fishes). In all these organisms, RVs cause severe diseases, including immunodeficiencies, neurological disorders, and different types of cancer, representing a major threat for all species; to date, no specific and effective treatments are available.² In addition, nonhuman RVs have been recently associated with human diseases by accidental infection, such as sporadic human breast cancer,³ or by ingestion of RV-infected meat (cattle and poultry), especially in immunocompromised individuals.⁴ Therefore, finding targets for therapeutic treatment of RVs is becoming an impellent issue.

The distinctive feature of RVs is retrotranscription of the two positive, single-stranded RNA genome filaments by the viral reverse-transcriptase (RT) enzyme; the generated double-stranded DNA is integrated into the host DNA to form the

provirus (Figure 1A). The proviral genome is next transcribed and translated to form new virions.⁵ When viral-genome integration occurs in somatic cells, RVs are classified as exogenous (XRVs); conversely, after occasional integration into the host germline and concurrent disruption of key viral genes, RVs may become endogenous (ERVs). XRVs are mainly organized into two subfamilies, Orthoretrovirinae and Spumavirinae, which differ in retrotranscription timing: the first includes six genera, namely alpha-, beta-, delta-, gamma-, and epsilon-RVs and lentiviruses, whereas the second comprises the spumavirus genus.²

The basic provirus organization is made of four coding genes, *gag*, *pro*, *pol*, and *env*, flanked by two identical untranslated regions, the long terminal repeats (LTRs, Figure 1B). Complex RVs also contain additional genes encoding for accessory proteins. The 5'-LTR is the control center for retroviral gene expression, consisting of three sections, U3, R,

Received: January 13, 2019

Published: May 13, 2019

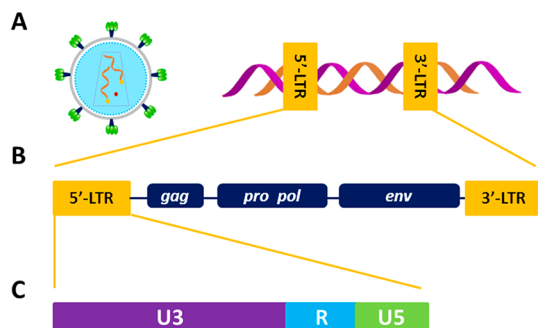


Figure 1. RV structure and genome organization. (A) Simplified model of an RV virion (left) and of the integrated provirus (right). (B) RV-provirus organization. (C) Regions of the 5'-LTR promoter.

68 and U5 (Figure 1C). The U3 region, which includes binding
69 sites for transcription factors, represents the RV-unique
70 promoter.⁶ In human immunodeficiency virus type 1 (HIV-
71 1), we demonstrated that the LTR-U3 guanine (G)-rich region
72 adopts noncanonical secondary structures, namely, G-quad-
73 ruplexes (G4s).⁷ G4s may form within G-rich strands of
74 nucleic acids when four Gs are linked together through
75 Hoogsteen-type hydrogen bonds to assemble in self-stacked G-
76 tetrads coordinated by monovalent cations.⁸ In HIV-1, the
77 fine-tuning of G4 structures due to cellular proteins has been
78 directly correlated to the regulation of viral transcription:
79 stabilization and unfolding of G4s silence and promote
80 transcription, respectively.^{9,10} Moreover, G4 ligands strongly
81 reduce virus propagation.^{11,12} Interestingly, despite the typical
82 great variability of the RV genomes, G-clusters in the LTR are
83 highly conserved in all primate lentiviruses.¹³ We observed that
84 the presence of G4s has been selected throughout evolution,
85 suggesting an active and central role in lentivirus biology. G4
86 correlation with transcription-factor binding sites suggests
87 exploitation of structural conserved elements as mechanosen-
88 sors in the regulation of key viral steps.¹³ In general,
89 bioinformatics studies traced putative G4-forming sequences
90 (PQSs) in almost all human viruses: most of these viral PQSs
91 are characterized by high degrees of conservation and
92 statistically significant distributions, implying essential bio-
93 logical roles.¹⁴ Altogether, these findings show that despite the
94 large mutation rates of viruses, G4s represent key elements in
95 the viral life cycle and consequently are interesting targets in
96 the development of innovative drugs.

In this context, with the purpose of examining the presence
97 and role of G4s in the retroviral machinery and of ultimately
98 identifying new targets for antiretroviral therapy, here we
99 sought to investigate the G4 distribution and conservation in
100 the whole Retroviridae family, and we present a comprehensive
101 analysis of G4s within the RV genomes. Using genomewide
102 bioinformatic analysis, we show that all RV genera contain
103 PQSs. PQSs in the 5'-LTR promoter were focused on and
104 investigated for their ability to actually fold into G4s. We
105 demonstrate that, despite plentiful differences among RVs, G4s
106 in regulatory regions represent a feature common to all genera.
107

RESULTS

108

Putative Quadruplex-Forming Sequences (PQSs) in the LTR-Promoter Regions of Most RVs. We initially
109 investigated the presence of PQSs in the full-length genomes of
110 all RVs, with the exception of lentiviruses as that genus had
111 been previously examined for the presence of G4s.¹³ Analysis
112 was performed using the QuadBase2 web server,¹⁵ which
113 allows flexible customization of loop length and inclusion of
114 bulges, as some G4s have been reported to form even in the
115 presence of noncontinuous Gs within G-runs.^{16,17} We searched
116 for sequences located in both the forward and reverse strands
117 of the RV integrated genomes characterized by (i) at least 3 Gs
118 in each run, (ii) continuous or 1-nucleotide-bulged G-runs,
119 and (iii) 1 to 12 nucleotide-long loops (G₃L₁₋₁₂). All the
120 viruses investigated in this study are listed in Table S1.
121

PQSs were observed in all RV genera, for a total of 1050
122 sequences over 48 analyzed viruses (Figure 2A). The average
123 number of observed PQSs per genus ranged from 7 to 48.
124 Delta-RVs were particularly enriched in PQSs, with very low
125 variability among viruses; conversely, epsilon- and spuma-RVs
126 showed 7- and 5-fold lower PQS amounts, respectively. Alpha-,
127 beta-, and gamma-RV genera displayed great variability among
128 the different viruses, with average PQSs-per-virus values of 20,
129 15, and 26, respectively.
130

We previously observed that G4s in the LTR of the HIV-1
131 provirus act as regulators of viral transcription.⁷ The presence
132 and pattern of G4-forming sequences is extremely conserved in
133 all primate lentiviruses,¹³ thereby pointing toward a key
134 regulatory role of LTR G4s in the whole lentivirus genus.
135 Consequently, we here focused our analysis on the LTR region
136 of RVs: LTR PQSs were found in all RV genera, except for the
137 epsilon-RVs, for a total of 65 PQSs over 48 analyzed viruses;
138 delta-RVs were confirmed to be the most enriched in PQSs
139
140

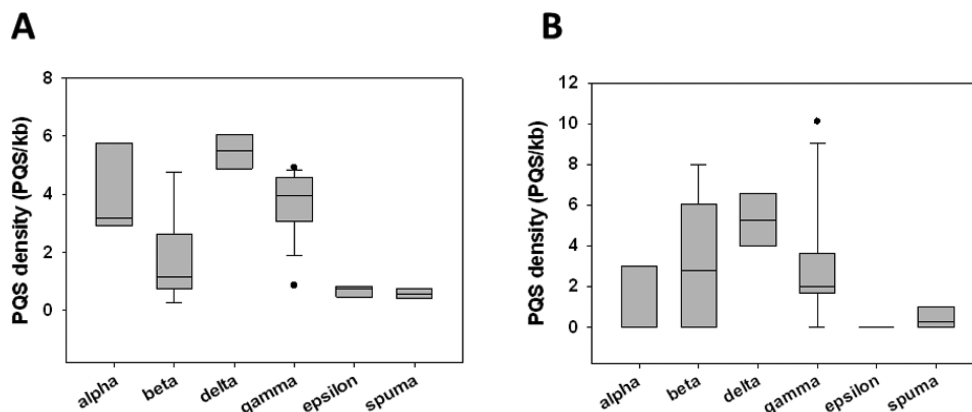


Figure 2. Box plots showing average PQS densities (PQS/Kb) in full-length genomes (A) and LTR regions (B) of RVs.

141 among all genera (Figure 2B). About 80% of the PQSs (50 out
142 of 65) were located in the reverse strand. All found sequences
143 are reported in Table S2.

144 We also observed that the majority of PQSs (~70%) were
145 located in the U3 region, just upstream of the transcription
146 start site (Figure 3). The U3 region plays a crucial role in the

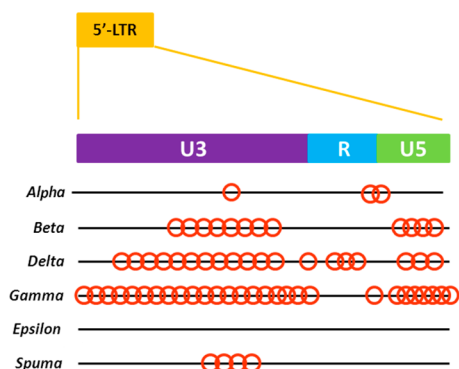


Figure 3. PQS distribution along the LTR regions of RVs. Each red circle indicates one PQS.

induction of viral transcription, as it comprises the unique promoter and transcription-factor binding sites: in this regard, we have proved that G4 sequences significantly overlap with Sp1 binding sites in the HIV-1 and primate lentiviruses.¹³

From this first screening, sequences containing more than one bulged G-tract were excluded, as the presence of too many bulged G-tracts has been reported to reduce G4 stability and even prevent their formation.¹⁸ Consequently, 29 sequences were obtained, distributed as follows: 8 in the beta-RV genus, 6 in the delta-RV genus, and 15 in the gamma-RV genus (Table 1). The observed sequences greatly varied in terms of length (22–44 nucleotides) and number of G-tracts (4–6). However, similarities were found in Mo-MLV and MuSV RVs, where the RV16 and RV29 sequences had the same base composition, and RV15 and RV28 differed by just three nucleotides in the last G-tract. Six sequences comprised continuous G-tracts, whereas the remaining 23 contained a bulged G-tract. Moreover, loop composition was quite mixed, as the sequences included very short loops ($L \leq 5$ nt, in RV4, RV7, RV9, RV12, RV18, and RV21) and very long ones ($9 < L < 12$ nt in RV15 and RV25), whereas the remaining presented miscellaneous loop organization.

Table 1. PQS Analysis Performed with QuadBase2 within the LTR Regions of RVs^a

	Virus	Name	Sequence	Strand ^b
Beta-RVs	DrERV	RV1	GGGCAGCGCTGCACT GCGG AGGAGGGGTGAGGAGGG	-
	ENTV-1	RV2	<u>GC</u> GGGGG ACAACCT GCGG AGGGTTAAGTCCT GGG AG	+
	SMRV	RV3	GGGCGT GGT GCG GGG CCACCAAT GGAG GACCTGATCAC GGG	+
		RV4	GGGTTCTTATATAGGGAGGGGAGAGGGTAGAGAGGGG	-
	MPMV	RV5	GGAG <u>GA</u> GGG AGT GGG AATTGAAGGG	-
	MMTV	RV6	GGGGCTATT GGGG GAAGTT GCGG TTTCGTGCTCGCAGGG	+
		RV7	<u>GA</u> GGG TCACC GGGG TCT GCGG GGGG	-
	SRV-4	RV8	<u>GGC</u> GGG AAGGAA GGG AAACGTCA GCGG ACGCT GGG	-
Delta-RVs	STLV-2	RV9	GGGCCA G T G TGCAGGGAGGGG	-
		RV10	GGGTGTTTT GGG CCCTCTCC GGG AGGGG	+
	HTLV-2	RV11	GGGGGA GGG ACGTCA GGG CC GTGG	-
		RV12	GGGGAAGT GCG TAA GGG TAGG	-
		RV13	GCGC TCCC GGGG CCAACATACGCC GTGG AGCGCAGCAA GGG CTA GGG	+
	BLV	RV14	GGGT G T G GATTTTT GGG AAA GGG GAAGTT GGG AGGTAC GGGG	-
Gamma-RVs	MoMLV	RV15	GGGGTCTTTTCATTT GGGGG CTCGTCC GGG ATC GGG	+
		RV16	GGGACGTCTCC AGGG TT GCGG CC GGG TG	-
		RV17	GGGAGACGTCC AGGG ACTTC GGGGG CCGTTTTT GTGG	+
	BaEV	RV18	GGGTCT GGG TTGC GCGG TC GGG	-
		RV19	GGGGT GGG ATAG GTG CTAGCCCC GGGG AGGTCT GGGG	-
	Mus	RV20	GGGACA GGGG CCAAATAT GGTG GTCAAGCACCT GGG	+
		RV21	GGGTAT GGGA GGGG TAC GAGG AAA GGG	-
		RV22	GGGCT GGGG CT GGGG AGCAAAAAG GCGG	-
	RD-114	RV23	GCGG CT GGGG ACTTTCCGGCTA GGG T GGGG CGCATAA GCGG	-
		RV24	GGGTTGCGAA GCGG CTGATGCAACT GGGG CC GGG	-
		RV25	G T G T G TT GGGG TTGT GGG TAATTTTCGTCCC GGGG AAGCTT GGG	-
	REV	RV26	<u>GT</u> GGG AGGGAGCTCC GGGG GGGG	-
	MuSV	RV27	GAGG CTTTATT GGG AATAC GGG TACCC GGG CG	-
	RV28	GGGGTCTTTTCATTT GGGG GCTCGTCC GGG ATT GGAG	+	
	RV29	GGGACGTCTCC AGGG TT GCGG CC GGG TG	-	

^aG₃ tracts are shown in red and bold, nonoverlapping bulged G₃ tracts (e.g., GGXG) are shown in blue and bold, and overlapping bulged G₃ tracts (e.g., GXGGG) are underlined. ^bPQS location: “+” indicates the forward strand, and “-” indicates the reverse strand.

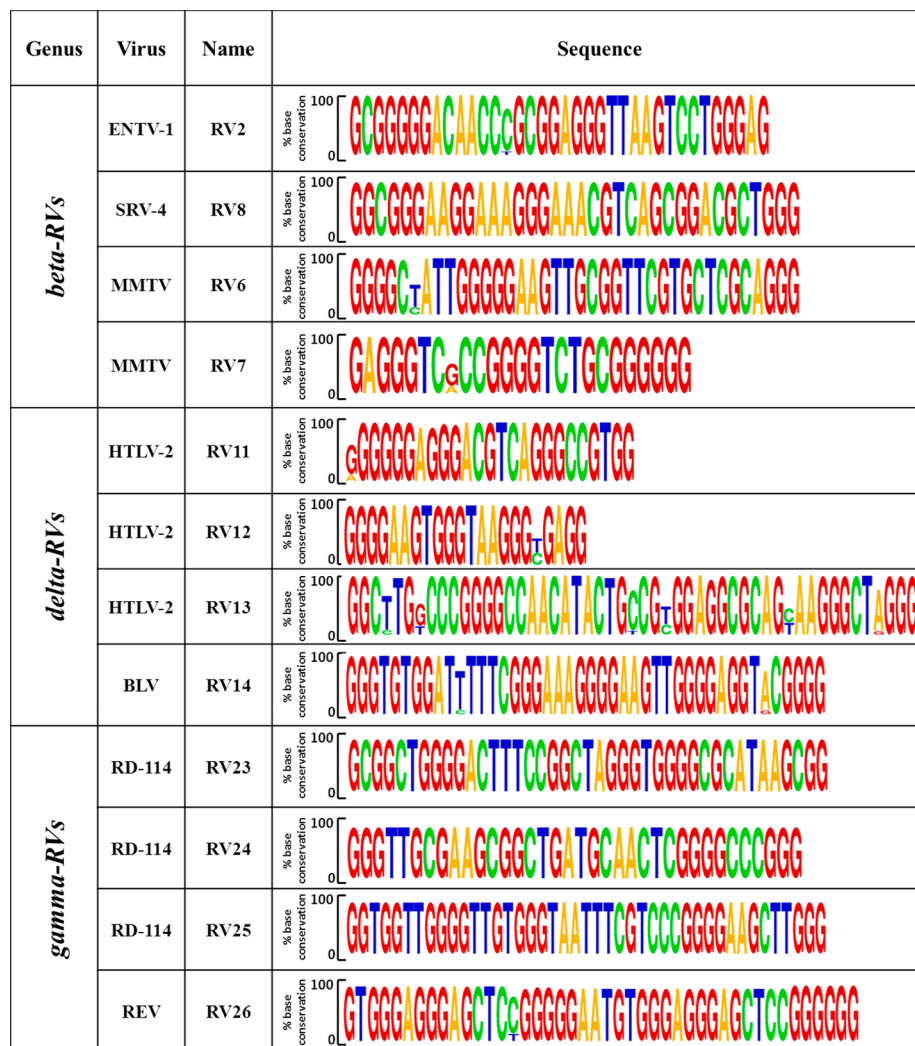


Figure 4. Base conservation of putative G4-forming sequences within strains of each RV species. Consensus sequences were obtained by alignment of at least five sequences.

169 **Highly Conserved PQSs in RV LTRs.** To assess the
 170 relevance of PQSs, we performed base-conservation analysis.
 171 Generally, RVs show high genetic variability, mainly as a result
 172 of error-prone proviral-genome synthesis and recombination
 173 between the two RNA copies during retrotranscription.¹⁹
 174 Nonetheless, conservation analysis, conducted on all RVs for
 175 which five or more complete LTR sequences were available
 176 (Table S3), showed an extremely high degree of G-base
 177 conservation, especially within G-tracts that are likely involved
 178 in G4 formation (Figure 4). These results corroborate the data
 179 obtained for lentiviruses¹³ and herpesviruses,^{20–22} further
 180 suggesting that G4s are key elements in the viral cycle and
 181 therefore have been selected for during viral-genome evolution.

182 **RV-LTR-PQS Folding into G4.** The actual ability of PQSs
 183 to fold into G4s was initially ascertained by circular-dichroism
 184 (CD) spectroscopy, as signature CD spectra are available for
 185 G4s.²³ Representative CD spectra showing a G4 RV, a non-G4
 186 RV and two different mixed G4 RVs are shown in Figure 5;
 187 CD spectra of all the analyzed sequences and their melting
 188 profiles are reported, organized by genus, in Figures S1–S4.
 189 Most of the examined oligonucleotides displayed clear-cut G4
 190 signatures, such as RV26 (Figure 5A) and RV5 and RV7
 191 (Figure S1). The majority of the sequences, however, were
 192 characterized by complex CD profiles (Figures 5C,D and S1–

S4), likely indicating the coexistence of multiple conforma-
 193 tions, corroborating the high dynamism and polymorphism
 194 reported for G4 DNA structures. RV3, for instance, showed
 195 two different transitions at 260 and 290 nm (Figure 5C),
 196 which may indicate the contribution of a parallel and an
 197 antiparallel conformation, respectively.²³ Five sequences, RV2,
 198 RV6, RV8, RV13, and RV27, displayed a broad peak in the
 199 260–280 nm wavelength range, indicating a prevalent non-G4
 200 conformation (Figures 5B, S1, S2, and S4).²⁴ We also
 201 evaluated the effects of two different compounds, BRACO-
 202 19 (B19, compound 1, Figure 6) and a core-extended
 203 naphthalenediimide (c-exNDI, compound 2, Figure 6), on RV
 204 G4 topology. Both molecules have been employed as G4
 205 ligands in viruses:²⁵ 1 has been reported to inhibit HIV-1 both
 206 in lytic and latent infections,^{11,26} and 2 has been shown to
 207 preferentially bind and stabilize viral G4s over cellular
 208 ones.^{12,27} CD experiments were conducted in the presence
 209 of 4 equiv of compounds and showed diverse effects: in the
 210 case of the RV3 sequence, for example, 1 strongly increased the
 211 molar ellipticity at 260 nm, suggesting the preferential binding
 212 for one of the possible conformations. In contrast, 2 enhanced
 213 the peak at 290 nm, providing a different CD spectrum (Figure
 214 5C). Peculiar effects were also observed for other sequences:
 215 for example, in RV9, in which the peaks at 260 and 290 nm
 216

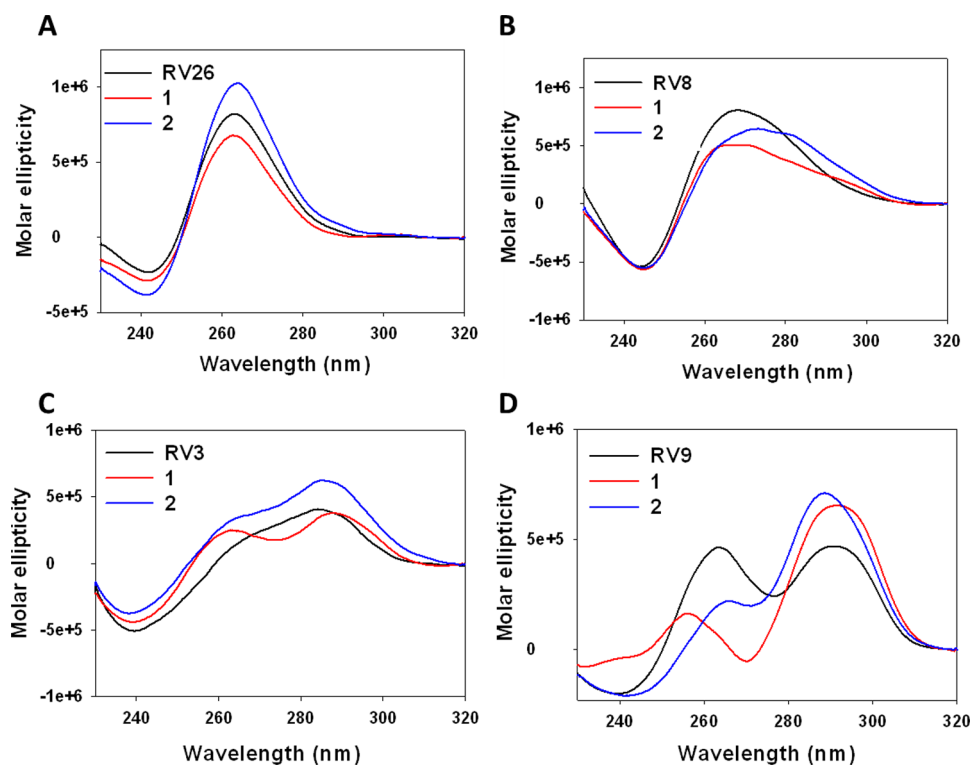


Figure 5. Representative CD spectra of RV G4 sequences in the absence (black line) or presence of G4 ligands 1 (red line) and 2 (blue line). (A) G4 CD spectrum, characterized by a maximum peak at $\lambda = 260$ nm and a minimum one at $\lambda = 240$ nm, which define a parallel conformation. (B) Non-G4 CD spectrum, characterized by a broad signal at $260 < \lambda < 280$ nm. (C–D) Two different mixed-G4 CD profiles.

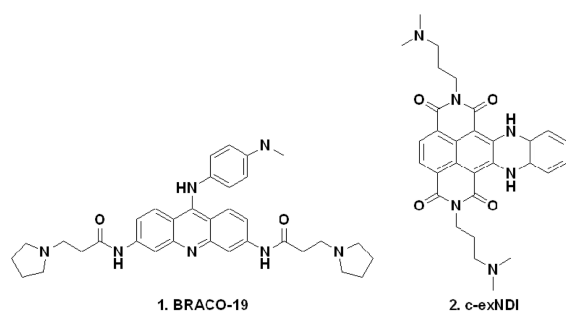


Figure 6. Chemical structures of the G4 ligands B19 (1) and c-exNDI (2) employed in this study.

display similar intensities, **1** totally abolished the peak at 260 nm, whereas **2** enhanced both transitions (Figure S4). Such structure-related behaviors imply that the two compounds may exert their G4 stabilizing activities through different binding modes.

To evaluate the stability of the RV G4s, we next performed CD thermal-denaturation experiments in the temperature (T) range of 20–95 °C. RV26 was the most stable G4, with a melting temperature (T_m) of 74.3 °C, whereas the least stable was RV24 ($T_m = 41$ °C). Moreover, plotting of the molar ellipticity versus T revealed two major melting transitions for hybrid G4s, at $\lambda = 260$ and 290 nm, the T_m of which are reported in Table 2. The occurrence of multiple melting transitions confirms the coexistence of different conformations in solution, each characterized by different T_m values. In some cases, such as with the RV9 sequence, two very clear transitions and thus T_m values were obtained, whereas in the

other case, such as with RV3, the presence of different species was so complex that it precluded the determination of single T_m values. In general, all G4-forming sequences displayed $T_m > 37$ °C, suggesting that RV G4s can stably fold in conditions that are close to the physiological ones. CD melting analysis in the presence of compounds showed a general stabilization effect on G4s, the T_m values of which were generally enhanced after G4-ligand treatment (Table 2). The different effects induced by the two compounds on the different RV G4s suggest the existence of different G4-binding mechanisms.

Dimethylsulfate (DMS)-footprinting analysis was next carried out to evaluate the G bases involved in G4 formation. We selected seven representative sequences, according to the folding characteristics observed in CD analysis: RV26, RV7, and RV5 for the parallel conformation; RV18 for a predominant antiparallel topology; and RV9, RV22, and RV12 for mixed arrangements. Oligonucleotides were folded in the presence and absence of KCl and treated with DMS to analyze the G residues protected from DMS-induced methylation. In the absence of K⁺ ions, cleavage to all Gs was observed, suggesting an unstructured oligonucleotide form. On the other hand, in the presence of KCl, all analyzed sequences showed protection of three Gs in each G-tract, indicating their involvement in G4 formation. On the basis of the DMS-footprinting pattern, we propose that each analyzed RV G4 consists of three planar tetrads formed by four contiguous or bulged G-runs (Figure S5). Deeper investigation into the secondary arrangement could allow the design of specific ligands able to selectively bind the single RV G4s.

Stalling of Polymerase Progression by RV-LTR G4s.

To investigate whether the identified RV G4s were able to stall polymerase progression, a Taq-polymerase stop assay was performed. Eight RV G4-forming sequences, belonging to 266

Table 2. CD T_m Values of RV G4s in the Absence and Presence of G4 Ligands 1 and 2^a

		T_m (°C)			ΔT_m (°C)	
		—	1	2	1	2
beta-RVs	RV1	48.1 ± 0.9	68.9 ± 0.2	60.6 ± 0.8	20.8	12.5
	RV2	ND	ND	ND		
	RV3	ND	ND	ND		
	RV4	67.1 ± 1.2	>90	>90	>22.9	>22.9
	RV5	48.0 ± 1.9	68.9 ± 3.1	85.9 ± 1.2	20.9	37.9
		ND	ND	62.3 ± 1.1	ND	ND
	RV6	ND	ND	ND		
	RV7	63.9 ± 0.8	75.8 ± 0.9	>90	11.9	>26.1
delta-RVs	RV8	ND	ND	ND		
	RV9	65.1 ± 0.3	>90	>90	>24.9	>24.9
		64.9 ± 0.3	>90	>90	>25.1	>25.1
	RV10	66.4 ± 1.3	83.8 ± 2.1	>90	17.4	>20.6
		48.9 ± 0.8	72.1 ± 0.9	70.3 ± 2.5	23.2	24.4
	RV11	61.4 ± 0.3	79.2 ± 0.7	ND	14.6	ND
		56.6 ± 2.1	69.0 ± 3.8	63.4 ± 0.3	12.4	6.8
	RV12	63.1 ± 0.4	ND	ND	ND	ND
		63.3 ± 0.4	66.3 ± 0.1	66.9 ± 0.8	3.2	3.8
	RV13	ND	ND	ND		
	RV14	65.5 ± 0.8	>90	>90	>24.5	>24.5
	RV15	55.4 ± 0.1	>90	>90	>34.6	>34.6
gamma-RVs		ND	67.0 ± 0.1	62.1 ± 2.6	ND	ND
	RV16	ND	ND	ND	ND	ND
		53.3 ± 1.4	63.4 ± 1.0	68.5 ± 2.3	10.1	15.2
	RV17	52.3 ± 0.8	86.7 ± 1.0	57.0 ± 3.4	33.7	4.7
	RV18	59.9 ± 0.4	76.5 ± 0.1	70.6 ± 1.0	16.6	10.7
	RV19	66.8 ± 0.1	77.6 ± 0.6	85.1 ± 0.1	10.8	18.3
	RV20	ND	ND	ND		
	RV21	56.8 ± 0.1	ND	65.6 ± 1.8	ND	8.8
		56.1 ± 0.1	60.0 ± 2.4	69.6 ± 2.0	3.9	13.5
	RV22	54.2 ± 0.8	ND	ND	ND	ND
		54.7 ± 0.6	64.9 ± 2.9	75.9 ± 3.9	10.2	21.2
	RV23	56.9 ± 2.7	83.8 ± 3.9	81.4 ± 2.2	25	22.6
	RV24	41.2 ± 0.2	50.8 ± 0.1	43.9 ± 3.0	9.6	2.7
	RV25	53.4 ± 0.1	>90	>90	>35.6	>35.6
RV26	73.6 ± 0.6	>90	>90	>16.4	>16.4	
RV27	ND	ND	ND			
RV28	>90	>90	>90	ND	ND	
	ND	58.5 ± 4.5	71.0 ± 0.5	ND	ND	
RV29	ND	ND	ND	ND	ND	
	53.3 ± 1.4	63.4 ± 1.0	68.5 ± 2.3	10.1	15.2	

^aData are reported as mean values ± SD from at least two independent experiments. In cases of double transitions, T_m values calculated at $\lambda = 260$ nm (first value) and 290 nm (second value) are shown.

different genera and characterized by different G4 folding topologies and stability, were selected as reported above. Extended RV G4 templates (Table S4), containing primer-annealing sequences at the 3'-ends, were annealed to the primer (Table S4) and incubated with Taq polymerase for 30 min at the indicated temperature. The chosen sequences were investigated in the absence and presence of K^+ to establish G4 formation and in the presence of G4 ligands to assess ligand-induced G4 stabilization. The two investigated ligands were used at different concentrations (1 at 100 μ M and 2 at 100 nM), according to their previously observed activity.^{11,12} In the presence of 100 mM K^+ (Figure 7A, lane 2), all RV G4 templates stopped the polymerase at the most 3'-G-tract involved in G4 formation, indicating that K^+ stimulates G4 folding, which in turn blocks polymerase progression. Upon addition of G4 ligands, the intensity of the G4 stop bands

highly increased in all instances (Figure 7A, lanes 3 and 4), along with considerable reduction of the full-length amplicons, thus corroborating effective stabilization of the RV G4s by both compounds. In contrast, both ligands had no effect on a DNA template unable to fold into G4 (Figure 7A, non-G4 cnt, lanes 3 and 4), indicating that the observed polymerase inhibition was G4-dependent. Quantification of the stop sites corresponding to G4s and of the full-length products is shown in Figure 7B. Overall, these data are in line with those obtained by CD analysis and confirm the ability of the chosen sequences to fold into G4 and get stabilized by G4 ligands.

DISCUSSION

In the past few years, interest in the characterization of G4 structures and their role within viral genomes has greatly increased, providing new directions in the management of viral

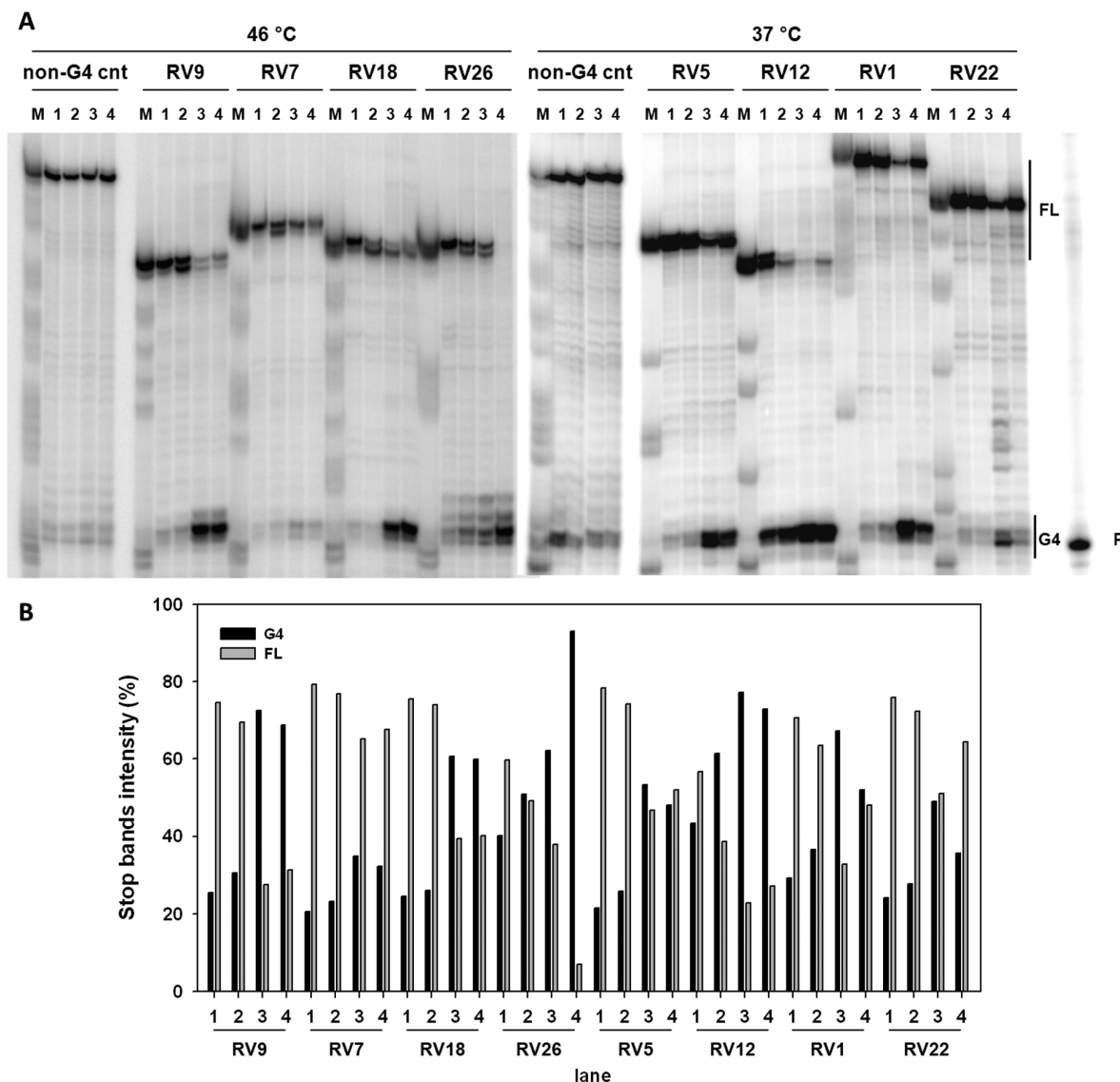


Figure 7. Representative Taq-polymerase stop assay of RV G4 sequences. (A) Templates amplified by Taq polymerase at the indicated temperature in the absence (lane 1) or presence of 100 mM K^+ alone (lane 2) or with G4 ligand 1 (lane 3) or 2 (lane 4). A template sequence (non-G4 cnt) made of a scrambled sequence unable to fold into a G4 was also used as an internal control. Lane P: unreacted labeled primer. Lane M: ladder of markers obtained by the Maxam and Gilbert sequencing protocol carried out on the amplified strand complementary to the template strand. Vertical bars indicate G4-specific Taq-polymerase stop sites. (B) Quantification of lanes shown in panel (A). Quantification of stop bands corresponding to G4 and of the full-length amplification product (FL) is shown.

298 infections. In this context, our group previously demonstrated
 299 that the HIV-1 transcription machinery is modulated by the
 300 tuned folding and unfolding of G4s located in the U3 region of
 301 LTR promoter. We proved that the G4 folding pattern is
 302 highly conserved not only among almost 1000 HIV-1 strains⁷
 303 but also among all primate lentiviruses,¹³ indicating G4s are
 304 crucial elements in viral evolution.

305 In this work, we investigated the presence of G4 structures
 306 in the whole Retroviridae family. In line with previously
 307 collected data on lentiviruses,¹³ we found PQSs in the LTRs of
 308 all RVs except for the epsilon-RVs. This last genus is the least
 309 represented, including only three virus species: it is tempting to
 310 speculate that the absence of G4s has impacted the evolution
 311 of this genus. As for the other RVs (the G4-containing RVs),
 312 we demonstrated that their PQSs (i) are well conserved, (ii)
 313 can actually adopt stable G4 arrangements, and (iii) are able to
 314 stall the polymerase enzyme.

In retrovirology, base-conservation analysis represents a
 critical issue, considering the high mutation rates of RVs. The
 limited availability of deposited sequences for most RVs
 hampers comprehensive conservation analysis; however, our
 data collected in this and previous works¹³ clearly indicate that
 G4-forming sequences are conserved elements within each RV
 LTR, thus representing essential elements for the virus life-
 cycle. Moreover, considering that all RV LTRs are charac-
 terized by the presence of PQSs, it may be hypothesized that,
 although LTRs greatly differ in terms of primary sequences and
 length, their shared functional homology could be ascribed to
 structural conserved elements like G4s.

The LTR is responsible for the expression of viral genes and
 ultimately for virus replication; it has been widely demon-
 strated that sequence variation in LTRs affects the binding of
 transcription factors, thus altering transcription.²⁸ Therefore,
 targeting the LTR may be effective in the treatment of

332 infections, and to this end, the employment of G4 ligands
333 represents a valuable approach. In this study, we demonstrated
334 that all RV-LTR G4s are stabilized in vitro by G4 binders and
335 that two different molecules stabilized a third of the selected
336 sequences by over 20 °C. Furthermore, the Taq-polymerase
337 stop assay revealed that this significant stabilization deeply
338 impacts polymerase progression. Notably, compounds 1 and 2
339 exerted comparable in vitro effects on the HIV-1 sequences
340 and, when tested in vivo, were able to greatly reduce virus
341 propagation.^{11,12} These data support the investigation of G4
342 ligands as promising candidates of innovative antiretroviral
343 drugs.

344 It is worth noting that development of anti-RV compounds
345 is currently limited to HIV. However, human-health-threat-
346 ening RVs are not restricted to lentiviruses; besides human
347 viruses like HTLV or HFV, there is an increasing body of
348 evidence that correlates nonhuman RVs with human diseases.
349 For example, the insurgence of sporadic human breast cancer
350 has been associated with MMTV infections;³ in addition,
351 immunocompromised people could be exposed to nutrition-
352 related RVs, like BLV or REV, which infect cattle and poultry,
353 respectively.^{4,29} The identification of structurally conserved
354 elements like G4s in RV genomes and the consequent
355 possibility to target them with specific compounds may thus
356 represent a turning point in the management of the widest
357 range of retroviral infections in humans and also in animal
358 species of interest, such as farm animals and pets.

359 An additional point of interest is that characterization of
360 LTR G4s has implications in genetics because 8% of the
361 human genome consists of LTR-transposable elements (TE),
362 including ERVs and single LTR segments, which have become
363 effective parts of the mammalian genome. A recent study
364 reported that G4s enrich the LTRs of plant TEs and human
365 ERVs, regulating transcription.^{30,31} The authors intriguingly
366 suggest that TEs could be the vehicles by which PQSs have
367 spread into the human genome.³² Considering that (i) LTRs
368 contain the majority of PQSs found in TEs,³² and (ii) LTR
369 elements in the human genome are derived from ancient RV
370 infections, RVs could represent the primordial organisms that
371 first developed G4 structures.

372 Our present work expands on the theme and substantiates
373 the consistent presence of G4s in LTR elements.

374 ■ CONCLUSIONS

375 The work proposed here provides a comprehensive overview
376 of the presence of G4s in RV-LTR-promoter regions. It adds to
377 the boosting recognition of G4s as widespread elements in the
378 broadest range of organisms, from higher to lower eukaryotes
379 and from plants to microorganisms.^{33–37} It follows that
380 research on G4s in viral LTRs has two implications: first, the
381 possibility to manage RV infections by developing innovative
382 drugs and, second, the opportunity to unravel the ancestral
383 mechanisms that regulate life as we know it today.

384 ■ EXPERIMENTAL SECTION

385 **Oligonucleotides and Compounds.** All the oligonucleo-
386 tides used in this work were purchased from Sigma-Aldrich
387 (Milan, Italy) and are listed in Tables 1 and S4. B19 was
388 obtained from ENDOTHERM (Saarbruecken, Germany), c-
389 exNDI was synthesized and kindly provided by Professor
390 Filippo Doria and Professor Mauro Freccero (University of
391 Pavia).

G4 Analysis of RV Genomes. Prediction of G4-forming
392 sequences on RV genomes and LTR regions was performed
393 using the QuadBase2 web server.¹⁵ The search was restricted
394 to G-tracts formed by 3 Gs (continuous or including 1
395 nucleotide bulge) and loops from 1 to 12 nucleotides.
396

**Base-Conservation Analysis of Predicted G4-Forming
Sequences.** Predicted G4-forming sequences were analyzed
397 in terms of base conservation by aligning sequences from
398 PubMed. Accession numbers of the whole set of sequences are
399 reported in Table S3. Conservation analysis was performed on
400 RVs with five or more sequences available in databases. LOGO
401 representation of base conservation was obtained by the
402 WebLogo software.³⁸
403

Circular-Dichroism Analysis. All the oligonucleotides
404 used in this study (Table 1) were diluted to final
405 concentrations of 3 μM in lithium cacodylate buffer (10
406 mM, pH 7.4) and KCl 100 mM. Samples were heated at 95 °C
407 for 5 min and then slowly cooled to room temperature. Where
408 indicated, compounds were added in 4 equiv, 4 h after
409 denaturation. CD spectra were recorded on a Chirascan-Plus
410 (Applied Photophysics, Leatherhead, U.K.) equipped with a
411 Peltier temperature controller using a quartz cell with a 5 mm
412 optical-path length. Thermal-unfolding experiments were
413 recorded from 230 to 320 nm over a temperature range of
414 20–90 °C. Acquired spectra were baseline-corrected for signal
415 contribution from the buffer, and the observed ellipticities were
416 converted to mean residue ellipticity according to $\theta = \text{degree} \times$
417 $\text{cm}^2 \times \text{dmol}^{-1}$ (mole ellipticity). T_m values were calculated
418 according to the van't Hoff equation applied for a two-state
419 transition from a folded state to an unfolded state
420

DMS-Footprinting Assay. Oligonucleotides were 5'-end-
421 labeled with [γ -³²P]ATP by T4 polynucleotide kinase (Thermo
422 Scientific, Milan, Italy) at 37 °C for 30 min and purified using
423 MicroSpin G-25 columns (GE Healthcare Europe, Milan,
424 Italy). They were next resuspended in lithium cacodylate buffer
425 (10 mM, pH 7.4) in the absence or presence of 100 mM KCl,
426 heat-denatured, and cooled to room temperature. Samples
427 were then treated with dimethylsulfate (DMS, 0.5% in ethanol)
428 for 5 min at room temperature, and the reaction was stopped
429 by the addition of 10% glycerol and β-mercaptoethanol before
430 the samples were loaded onto a 15% native polyacrylamide gel.
431 DNA bands were localized via autoradiography, excised, and
432 eluted in water overnight. The supernatants were recovered,
433 ethanol-precipitated, and treated with piperidine 10% solution
434 for 30 min at 90 °C. Reaction products were analyzed on 20%
435 denaturing polyacrylamide gels, visualized by phosphorimaging
436 analysis, and quantified by ImageQuant TL software (GE
437 Healthcare Europe, Milan, Italy).
438

Taq-Polymerase Stop Assay. The Taq-polymerase stop
439 assay was performed according to previously described
440 procedures.⁷ The labeled primer (final concentration of 72
441 nM) was annealed to the template (final concentration of 36
442 nM, Table S4) in lithium cacodylate buffer (10 mM, pH 7.4)
443 in the presence or absence of KCl 100 mM by heating at 95 °C
444 for 5 min. After gradual cooling to room temperature, the
445 samples were incubated, where indicated, with 1 (1 μM) or 2
446 (100 nM) at room temperature overnight. For primer
447 extension, AmpliTaq Gold DNA polymerase (2U per reaction;
448 Applied Biosystems, Carlsbad, CA) was employed at the
449 indicated temperature for 30 min. Reactions were stopped by
450 ethanol precipitation, and primer-extension products were
451 separated on a 16% denaturing gel and finally visualized by
452 phosphorimaging (Typhoon FLA 9000, GE Healthcare, Milan,
453

455 Italy). Markers were prepared on the basis of the Maxam and
456 Gilbert sequencing protocol.³⁹

457 ■ ASSOCIATED CONTENT

458 ● Supporting Information

459 The Supporting Information is available free of charge on the
460 ACS Publications website at DOI: 10.1021/acsinfec-
461 dis.9b00011.

462 Analyzed RVs, obtained sequences, accession numbers
463 of all RVs, oligonucleotide sequences used in the
464 biophysic assays, CD spectra, and DMS-footprinting
465 analysis (PDF)

466 ■ AUTHOR INFORMATION

467 Corresponding Author

468 *Tel.: +39 049 8272346. Fax: +39 049 8272355. E-mail: sara.
469 richter@unipd.it.

470 ORCID

471 Emanuela Ruggiero: 0000-0003-0989-4074

472 Sara N. Richter: 0000-0002-5446-9029

473 Author Contributions

474 E.R., M.T., R.P., and M.N. performed the experiments; S.N.R.
475 conceived the work; and E.R. and S.N.R. wrote the manuscript.
476 All authors have given approval to the final version of the
477 manuscript.

478 Notes

479 The authors declare no competing financial interest.

480 ■ ACKNOWLEDGMENTS

481 This work was supported by grants to S.N.R. from the
482 European Research Council (ERC Consolidator grant number
483 615879) and the Bill and Melinda Gates Foundation (grant
484 numbers OPP1035881 and OPP1097238).

485 ■ ABBREVIATIONS USED

486 RV, retrovirus; RT, reverse transcriptase; XRV, exogenous
487 retrovirus; ERV, endogenous retrovirus; LTR, long terminal
488 repeat; G4, G-quadruplex; PQS, putative G-quadruplex-
489 forming sequence; CD, circular dichroism; DMS, dimethyl
490 sulfate; TE, transposable element

491 ■ REFERENCES

492 (1) Hayward, A. (2017) Origin of the retroviruses: when, where, and
493 how? *Curr. Opin. Virol.* 25, 23–27.
494 (2) Greenwood, A. D., Ishida, Y., O'Brien, S. P., Roca, A. L., and
495 Eiden, M. V. (2018) Transmission, Evolution, and Endogenization:
496 Lessons Learned from Recent Retroviral Invasions. *Microbiol. Mol.*
497 *Biol. Rev.* 82, No. e00044-17.
498 (3) Braitbard, O., Roniger, M., Bar-Sinai, A., Rajchman, D., Gross,
499 T., Abramovitch, H., La Ferla, M., Franceschi, S., Lessi, F., Naccarato,
500 A. G., Mazzanti, C. M., Bevilacqua, G., and Hochman, J. (2016) A
501 new immunization and treatment strategy for mouse mammary tumor
502 virus (MMTV) associated cancers. *Oncotarget* 7, 21168–21180.
503 (4) Olaya-Galan, N. N., Corredor-Figueroa, A. P., Guzman-Garzon,
504 T. C., Rios-Hernandez, K. S., Salas-Cardenas, S. P., Patarroyo, M. A.,
505 and Gutierrez, M. F. (2017) Bovine leukaemia virus DNA in fresh
506 milk and raw beef for human consumption. *Epidemiol. Infect.* 145,
507 3125–3130.
508 (5) Jern, P., and Coffin, J. M. (2008) Effects of Retroviruses on Host
509 Genome Function. *Annu. Rev. Genet.* 42, 709–732.
510 (6) Wu, Y. (2004) HIV-1 gene expression: lessons from provirus and
511 non-integrated DNA. *Retrovirology* 1, 13.

(7) Perrone, R., Nadai, M., Frasson, I., Poe, J. A., Butovskaya, E.,
512 Smithgall, T. E., Palumbo, M., Palu, G., and Richter, S. N. (2013) A
513 dynamic G-quadruplex region regulates the HIV-1 long terminal
514 repeat promoter. *J. Med. Chem.* 56, 6521–6530. 515
(8) Rhodes, D., and Lipps, H. J. (2015) G-quadruplexes and their
516 regulatory roles in biology. *Nucleic Acids Res.* 43, 8627–8637. 517
(9) Tosoni, E., Frasson, I., Scalabrin, M., Perrone, R., Butovskaya, E.,
518 Nadai, M., Palu, G., Fabris, D., and Richter, S. N. (2015) Nucleolin
519 stabilizes G-quadruplex structures folded by the LTR promoter and
520 silences HIV-1 viral transcription. *Nucleic Acids Res.* 43, 8884–8897. 521
(10) Scalabrin, M., Frasson, I., Ruggiero, E., Perrone, R., Tosoni, E.,
522 Lago, S., Tassinari, M., Palù, G., and Richter, S. N. (2017) The
523 cellular protein hnRNP A2/B1 enhances HIV-1 transcription by
524 unfolding LTR promoter G-quadruplexes. *Sci. Rep.* 7, 45244. 525
(11) Perrone, R., Butovskaya, E., Daelemans, D., Palu, G.,
526 Pannecouque, C., and Richter, S. N. (2014) Anti-HIV-1 activity of
527 the G-quadruplex ligand BRACO-19. *J. Antimicrob. Chemother.* 69,
528 3248–3258. 529
(12) Perrone, R., Doria, F., Butovskaya, E., Frasson, I., Botti, S.,
530 Scalabrin, M., Lago, S., Grande, V., Nadai, M., Freccero, M., and
531 Richter, S. N. (2015) Synthesis, Binding and Antiviral Properties of
532 Potent Core-Extended Naphthalene Diimides Targeting the HIV-1
533 Long Terminal Repeat Promoter G-Quadruplexes. *J. Med. Chem.* 58,
534 9639–9652. 535
(13) Perrone, R., Lavezzo, E., Palù, G., and Richter, S. N. (2017)
536 Conserved presence of G-quadruplex forming sequences in the Long
537 Terminal Repeat Promoter of Lentiviruses. *Sci. Rep.* 7, 2018. 538
(14) Lavezzo, E., Berselli, M., Frasson, I., Perrone, R., Palù, G.,
539 Brazzale, A. R., Richter, S. N., Toppo, S., and LLexa, M. (2018) G-
540 quadruplex forming sequences in the genome of all known human
541 viruses: A comprehensive guide. *PLOS Comput. Biol.* 14,
542 No. e1006675. 543
(15) Dhapola, P., and Chowdhury, S. (2016) QuadBase2: web
544 server for multiplexed guanine quadruplex mining and visualization.
545 *Nucleic Acids Res.* 44, W277–W283. 546
(16) Meier, M., Moya-Torres, A., Krahn, N. J., McDougall, M. D.,
547 Orriss, G. L., McRae, E. K. S., Booy, E. P., McEleney, K., Patel, T. R.,
548 McKenna, S. A., and Stetefeld, J. (2018) Structure and hydrodynamics
549 of a DNA G-quadruplex with a cytosine bulge. *Nucleic Acids Res.* 46,
550 5319–5331. 551
(17) De Nicola, B., Lech, C. J., Heddi, B., Regmi, S., Frasson, I.,
552 Perrone, R., Richter, S. N., and Phan, A. T. (2016) Structure and
553 possible function of a G-quadruplex in the long terminal repeat of the
554 proviral HIV-1 genome. *Nucleic Acids Res.* 44, 6442–6451. 555
(18) Mukundan, V. T., and Phan, A. T. (2013) Bulges in G-
556 Quadruplexes: Broadening the Definition of G-Quadruplex-Forming
557 Sequences. *J. Am. Chem. Soc.* 135, 5017–5028. 558
(19) Rethwilm, A., and Bodem, J. (2013) Evolution of Foamy
559 Viruses: The Most Ancient of All Retroviruses. *Viruses* 5, 2349–2374. 560
(20) Biswas, B., Kandpal, M., Jauhari, U. K., and Vivekanandan, P.
561 (2016) Genome-wide analysis of G-quadruplexes in herpesvirus
562 genomes. *BMC Genomics* 17, 949. 563
(21) Artusi, S., Nadai, M., Perrone, R., Biasolo, M. A., Palu, G.,
564 Flamand, L., Calistri, A., and Richter, S. N. (2015) The Herpes
565 Simplex Virus-1 genome contains multiple clusters of repeated G-
566 quadruplex: Implications for the antiviral activity of a G-quadruplex
567 ligand. *Antiviral Res.* 118, 123–131. 568
(22) Biswas, B., Kumari, P., and Vivekanandan, P. (2018) *Pac1*
569 Signals of Human Herpesviruses Contain a Highly Conserved G-
570 Quadruplex Motif. *ACS Infect. Dis.* 4, 744–751. 571
(23) Vorlíčková, M., Kejnovská, I., Sagi, J., Renčíuk, D., Bednářová,
572 K., Motlová, J., and Kypr, J. (2012) Circular dichroism and guanine
573 quadruplexes. *Methods* 57, 64–75. 574
(24) Kypr, J., Kejnovska, I., Renciuk, D., and Vorlickova, M. (2009)
575 Circular dichroism and conformational polymorphism of DNA.
576 *Nucleic Acids Res.* 37, 1713–1725. 577
(25) Ruggiero, E., and Richter, S. N. (2018) G-quadruplexes and G-
578 quadruplex ligands: targets and tools in antiviral therapy. *Nucleic Acids*
579 *Res.* 46, 3270–3283. 580

- 581 (26) Piekna-Przybylska, D., Sharma, G., Maggirwar, S. B., and
582 Bambara, R. A. (2017) Deficiency in DNA damage response, a new
583 characteristic of cells infected with latent HIV-1. *Cell Cycle* 16, 968–
584 978.
- 585 (27) Callegaro, S., Perrone, R., Scalabrin, M., Doria, F., Palu, G., and
586 Richter, S. N. (2017) A core extended naphthalene diimide G-
587 quadruplex ligand potently inhibits herpes simplex virus 1 replication.
588 *Sci. Rep.* 7, 2341.
- 589 (28) Krebs, F. C., Mehrens, D., Pomeroy, S., Goodenow, M. M., and
590 Wigdahl, B. (1998) Human Immunodeficiency Virus Type 1 Long
591 Terminal Repeat Quasispecies Differ in Basal Transcription and
592 Nuclear Factor Recruitment in Human Glial Cells and Lymphocytes.
593 *J. Biomed. Sci.* 5, 31–44.
- 594 (29) Gyles, C. (2016) Should we be more concerned about bovine
595 leukemia virus? *Can. Vet. J.* 57, 115–116.
- 596 (30) Kejnovsky, E., and Lexa, M. (2014) Quadruplex-forming DNA
597 sequences spread by retrotransposons may serve as genome
598 regulators. *Mob. Genet. Elements* 4, No. e28084.
- 599 (31) Lexa, M., Kejnovsky, E., Steflava, P., Konvalinova, H.,
600 Vorlickova, M., and Vyskot, B. (2014) Quadruplex-forming sequences
601 occupy discrete regions inside plant LTR retrotransposons. *Nucleic
602 Acids Res.* 42, 968–978.
- 603 (32) Kejnovsky, E., Tokan, V., and Lexa, M. (2015) Transposable
604 elements and G-quadruplexes. *Chromosome Res.* 23, 615–623.
- 605 (33) Griffin, B. D., and Bass, H. W. (2018) Review: Plant G-
606 quadruplex (G4) motifs in DNA and RNA; abundant, intriguing
607 sequences of unknown function. *Plant Sci.* 269, 143–147.
- 608 (34) Vinyard, W. A., Fleming, A. M., Ma, J., and Burrows, C. J.
609 (2018) Characterization of G-Quadruplexes in *Chlamydomonas*
610 *reinhardtii* and the Effects of Polyamine and Magnesium Cations on
611 Structure and Stability. *Biochemistry* 57, 6551–6561.
- 612 (35) Harris, L. M., Monsell, K. R., Noulin, F., Famodimu, M. T.,
613 Smargiasso, N., Damblon, C., Horrocks, P., and Merrick, C. J. (2018)
614 G-Quadruplex DNA Motifs in the Malaria Parasite Plasmodium
615 falciparum and Their Potential as Novel Antimalarial Drug Targets.
616 *Antimicrob. Agents Chemother.* 62, No. e01828-17.
- 617 (36) Guédin, A., Lin, L. Y., Armane, S., Lacroix, L., Mergny, J.-L.,
618 Thore, S., and Yatsunyk, L. A. (2018) Quadruplexes in “Dicty”: crystal
619 structure of a four-quartet G-quadruplex formed by G-rich motif
620 found in the Dictyostelium discoideum genome. *Nucleic Acids Res.* 46,
621 5297–5307.
- 622 (37) Turturici, G., La Fiora, V., Terenzi, A., Barone, G., and
623 Cavalieri, V. (2018) Perturbation of Developmental Regulatory Gene
624 Expression by a G-Quadruplex DNA Inducer in the Sea Urchin
625 Embryo. *Biochemistry* 57, 4391–4394.
- 626 (38) Crooks, G. E., Hon, G., Chandonia, J.-M., and Brenner, S. E.
627 (2004) WebLogo: A Sequence Logo Generator. *Genome Res.* 14,
628 1188–1190.
- 629 (39) Maxam, A. M., and Gilbert, W. (1980) [57] Sequencing End-
630 Labeled DNA with Base-Specific Chemical Cleavages. *Methods*
631 *Enzymol.* 65, 499–560.